Data Power Management for the Downlink of Multibeam MIMO Systems Serving Ground Users and Uncrewed Aerial Vehicles

Sezanildo da S. P. Filho, Vitória Hellen F. Coelho, Maria Clara R. Lobão, Roberto P. Antonioli, Yuri C. B. Silva and Walter C. Freitas Jr.

***Abstract*— In the context of sixth-generation (6G) architectures, multiple input multiple output (MIMO) networks emerged with innovative proposals for the future of mobile communications with various applications. Among the many applications, the integration of uncrewed aerial vehicles (UAVs) and ground users (GUEs), combined with the multibeam technique stands out as a powerful alternative for efficiently transmitting and receiving signals. In this article, we study the downlink communication between an access point and a mixture of cellular users, comprised of UAVs and GUEs. The access point employs a multibeam technique to steer beams towards UAVs and GUEs to improve the communication, while also performing power management in the beamforming vectors as a key element. Our results indicate that the variation in the power allocation of the multibeams has a direct impact on the performance of network users. This suggests a wide range of applications in the future prospects for mobile networks.**

***Keywords*— MIMO, UAV, multibeam, power allocation.**

I. INTRODUCTION

In recent decades, we have witnessed an astonishing development of wireless systems, a growth that has allowed the validation of a variety of applications. In this specific context, the development of mobile networks has emerged as a major protagonist, allowing users to have increasingly faster connections, providing innovative services according to current needs. However, as the demand for mobile services continues to grow, especially in densely populated urban environments, new technical challenges arise that require equally innovative and efficient solutions.

In the scenario of sixth generation systems (6G), a promising approach to solving these new challenges is the integration of multibeam systems in multiple input multiple output (MIMO) networks. MIMO networks are characterized by their high scalability, offering very high data rate and stable connections. In the configuration of these networks, base stations are equipped with numerous antennas that serve multiple single-antenna terminals simultaneously, concentrating power in a compact spatial area, effectively mitigating interference. This strategy improves energy efficiency and minimizes latency [1]. By combining multibeam technologies, which enable adaptive targeting of signals to specific users, we can create a highly adaptable and scalable communications infrastructure essential to meeting the growing demands of mobile networks.

Given the new perspectives of the next generation, a research field that has been gaining prominence is the integration of uncrewed aerial vehicles (UAVs) in mobile networks. UAVs are recognized as the ideal choice to make more efficient and automate operations such as: search and rescue, crowd supervision and management and meteorological monitoring [2]. By combining this integration with multibeam and power allocation technologies, we can obtain a network which can be used to meet specific communication needs, also implying improvements in terms of resource efficiency in wireless communication systems.

Considering MIMO systems that serve both ground users (GUEs) and UAVs, the authors in [1] have explored the potential of massive MIMO for UAVs. They analyzed maximizing transmission capacity and developed a realistic model accounting for polarization losses due to UAV movement, as well as determining optimal antenna spacing to improve transmission rates. In [2], cellular communication with UAVs was examined emphasizing the command and control (C&C) channel's importance for aerial users, which is vital for the technology's commercial success. In the context of cell-free systems serving both GUEs and UAVs, [3] has investigated methods to serve both GUEs and UAVs by adapting the antenna tilting. In [4], power allocations and user scheduling for the uplink and downlink of cell-free systems with UAVs and GUEs were examined. However, none of the above studies investigated multibeam approaches for simultaneously serving GUEs and UAVs.

In this study, we investigate the application of multibeam transmission in MIMO systems, seeking to jointly serve both the ground users (GUE) and the UAVs, which are types of users with very different propagation characteristics. Our proposal consists of directing beams to the terrestrial users and to the UAVs, wich are then combined by properly managing the power allocation among these beams. The main objective of this work is to compare the signal-to-interference-plus-noise ratio (SINR) metrics of these two types of users when beam direction and power adjustments are made.

This article is organized as follows. In the second section, the system model is presented. The third section discusses

Sezanildo da S. P. Filho, Maria Clara R. Lobão, Roberto P. Antonioli, Yuri C. B. Silva, Walter C. Freitas Jr. are with the Wireless Telecommunications Research Group (GTEL), Federal University of Ceará (UFC), Fortaleza, Brazil. E-mails: {seza, clara, antonioli, yuri, walter}@gtel.ufc.br. Vitória Hellen F. Coelho is with Federal University of Ceara (UFC), Fortaleza, Brazil. E-mail: vitoriafeitosa@alu.ufc.br. This work was supported in part by the Brazilian National Council for Scientific and Technological Development (CNPq) Proc. no. 409228/2021-4, in part by Ericsson Research, Technical Cooperation Contract UFC.50.

the beamforming design and power allcation strategy for the multibeam system. The fourth section provides an analysis of the results, obtained by means of computer simulations. Finally, the last section presents the conclusions and future perspective.

II. System Model

A. Network architecture

In this article, we consider a network architecture based on [3]. Our scenario consists of an access point (AP) serving UAVs and GUEs, as illustrated seen in Fig. 1. In the network, the numbers of UAVs and GUEs are defined as M_{uav} and M_{gue}, respectively. The total number of users in the system is $M = M_{uav} + M_{gue}$. The AP is connected to a central processing unit (CPU) through fronthaul links. The system operates using a time division duplex (TDD) protocol, with a focus solely on evaluating the downlink (DL) transmission. The considered geographical area is arranged in a square grid with dimensions of 200 m × 200 m. We make the assumption that the UAVs and GUEs possess only one antenna, while the AP serves the users with an array comprised of N antenna elements.

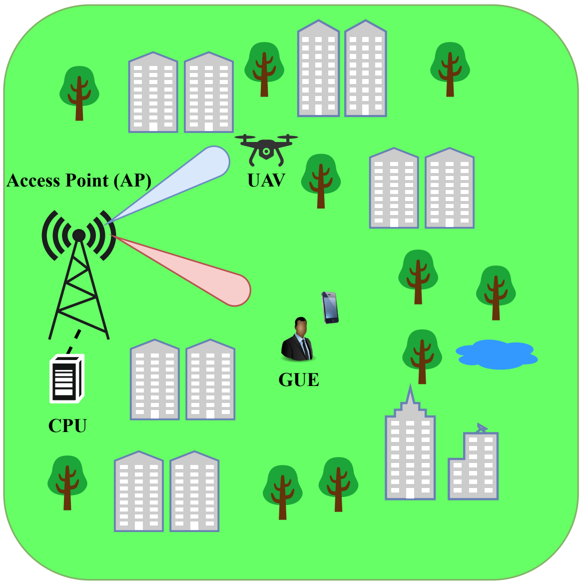

Fig. 1: Proposed scenario.

B. Signal model

In our downlink scenario, we have an access point equipped with a uniform linear array (ULA) with N antenna elements, which transmit data from independent symbols to M single-antenna users. The signal $\mathbf{x} \in \mathbb{C}^{N\times 1}$ transmitted to the M users from the antenna array can be represented by:

$$\mathbf{x} = \mathbf{W}\Lambda\mathbf{s}, \tag{1}$$

where $\mathbf{W} \in \mathbb{C}^{N\times M}$ is the matrix containing the beamforming vectors, $\mathbf{s} \in \mathbb{C}^{M\times 1}$ is the vector that contains the baseband signals of all users and $\Lambda^{M\times M}$ is defined as:

$$\Lambda \triangleq \begin{bmatrix} \sqrt{\rho_1} & 0 & \cdots & 0 \\ 0 & \sqrt{\rho_2} & \cdots & 0 \\ \vdots & \vdots & \ddots & \vdots \\ 0 & 0 & \cdots & \sqrt{\rho_M} \end{bmatrix}, \tag{2}$$

where ρ_m, with $m = 1, \ldots, M$, determines the power allocated to the beamforming designed for user m (either GUE or UAV).

The signal received by the m-th user, either UAV or GUE, can be formulated as:

$$y_m^{dl} = \underbrace{\sqrt{\rho_m}\mathbf{g}_m^T\mathbf{w}_m s_m}_{\text{desired signal}} + \underbrace{\sum_{\substack{j=1\\ j\neq m}}^{M} \sqrt{\rho_j}\mathbf{g}_m^T\mathbf{w}_j s_j}_{\text{interference}} + n_m, \tag{3}$$

where $\mathbf{g}_m \in \mathbb{C}^{N\times 1}$ is the channel vector, n_m is the additive white Gaussian noise with variance σ_m^2 at the m-th user and $\mathbf{w}_m \in \mathbb{C}^{N\times 1}$ is the beamforming vector used by the AP to transmit to the m-th user (UAV or GUE). Thus, assuming symbols with unit variance, it is possible to calculate the SINR as follows:

$$\gamma_m^{dl} = \frac{|\mathbf{g}_m^T\mathbf{w}_m|^2\rho_m}{\sum_{\substack{j=1\\ j\neq m}}^{M} |\mathbf{g}_m^T\mathbf{w}_j|^2\rho_j + \sigma_m^2}. \tag{4}$$

To ensure a maximum transmission power at the AP, we consider the following constraint on the transmit power values used by the AP:

$$\mathbb{E}\{||\mathbf{W}\Lambda\mathbf{s}||^2\} \leq P_t, \tag{5}$$

Applying the trace operation and knowing that the expectation and trace are linear operators, we arrive at:

$$\mathrm{tr}(\mathbf{W}^H\mathbf{W}\Lambda\Lambda^H) \leq P_t, \tag{6}$$

where P_t is the power budget for the AP. If we assume unit-norm beamforming vectors, the power constraint can be further simplified to:

$$\textstyle\sum_{m=1}^{M} \rho_m \leq P_t. \tag{7}$$

C. Propagation model

Similarly as in [5], we describe the small-scale fading phenomenon using a Ricean fading model, which encompasses line-of-sight (LOS) and non-line-of-sight (NLOS) components. The communication channel $\mathbf{g}_m \in \mathbb{C}^{N\times 1}$ between the AP and the m-th user is characterized by the following expression:

$$\mathbf{g}_m = \sqrt{\frac{\beta_m}{K_m + 1}}\left[\sqrt{K_m}\mathbf{a}(\theta_m, \phi_m) + \mathbf{h}_m\right], \tag{8}$$

where K_m represents the Ricean K-factor, $\mathbf{h}_m \in \mathbb{C}^{N\times 1} \sim \mathcal{N}(0, \mathbf{R}_m)$, represents the non-line-of-sight (NLOS) Rayleigh term, $\mathbf{R}_m \in \mathbb{C}^{N\times N}$ is the channel spatial correlation matrix, and $\mathbf{a}(\theta_m, \phi_m) \in \mathbb{C}^{N\times 1}$ denotes the steering vector (defined in Section II-E) with respect to the m-th user.

The probability of LOS for the link between the users and the AP follows the model defined in [6] and [7]. This value is directly associated with the horizontal distance between the users and the base station. Given the probabilities, we can determine the K-factor, which can be seen in Table I, and also the path-loss model by following the specifications for UAVs and GUEs for urban micro scenario (UMi) given also in [6] and [7], respectively.

TABLE I:
K-FACTOR VALUES

USER	LOS	NLOS
UAV	15 dB	0
GUE	$\mathcal{N}(5,9)$ dB	0

The term β_m is the large-scale coefficient with respect to user m, which is given by [3]:

$$\beta_m = 10^{\frac{PL_m + SH_m + G_m}{10}}, \tag{9}$$

where PL_m is the path-loss model, SH_m represents the correlated shadowing and G_m is the receiver antenna gain with respect to user m. All values are in dB.

D. Radiation Pattern

The horizontal and vertical radiation pattern models were defined according to [3], [4], where the horizontal pattern is:

$$A(\theta) = -\min\left[12\left(\frac{\theta}{\theta_{3\text{dB}}}\right)^2, A_m\right]. \tag{10}$$

In this context, $A(\theta)$ stands for the relative antenna gain (measured in decibels) at the direction θ, where θ is the azimuth angle, where the incoming wave meets the receiving antenna, covering a range from $-180°$ to $180°$. The expression min signifies the minimum value, while $\theta_{3\text{dB}}$ refers to half-power beamwidth (HPBW), equivalent to $\theta_{3\text{dB}}= 70°$. Furthermore, $A_m = 20$ dB indicates the maximum attenuation.

For the vertical pattern, we have:

$$A(\phi) = -\min\left[12\left(\frac{\phi - \phi_{tilt}}{\phi_{3\text{dB}}}\right)^2, A_m\right]. \tag{11}$$

Here, $A(\phi)$ represents the relative antenna gain (in decibels) in the elevation direction ϕ, ranging from $-90° \leq \phi \leq 90°$. The value $\phi_{3\text{dB}}$ denotes the HPBW, typically assumed to be $15°$, and ϕ_{tilt} indicates the tilt angle.

By combining (10) and (11), we get [3]:

$$A(\theta, \phi) = -\min[-(A(\theta) + A(\phi)), A_m]. \tag{12}$$

E. Features of the antenna array

In the considered ULA arrangement configuration, the elements (antennas) are positioned along a straight line [8] evenly spaced in value of $d = (1/2)\lambda$, where λ is the wavelength. The steering vector $\mathbf{a}(\theta_m, \phi_m)$ is essentially a function of the angle of departure (AoD), which is given by:

$$\mathbf{a}(\theta_m, \phi_m) = [a_1, a_2, ..., a_n]^T, \tag{13}$$

and

$$a_n = e^{\frac{-j2\pi}{\lambda}(n-1)d\sin\theta_m\cos\phi_m}, \tag{14}$$

where θ_m and ϕ_m represents the azimuth and elevation AoDs, respectively, between the AP and the m-th user.

III. Beamforming Design and Power Allocation Strategy for Multibeam

The main goal of this work is to adopt a beamforming pattern that allows the AP to employ a multibeam approach and steer beams towards the UAVs and GUEs, while allocating the power for each beam, as described in [9]. To this end, the adopted strategy to compute $\mathbf{w}_m$ is given by [10]:

$$\mathbf{w}_m = \mathbf{a}(\theta_m, \phi_m), \tag{15}$$

where $\mathbf{a}(\theta_m, \phi_m)$ is the steering vector for user m. The values of θ_m and ϕ_m are assumed to have been previously estimated.

Using (15), the AP can balance the transmission power allocated to each user m by computing the matrix Λ. In this study, we analyze the cases in which the AP allocated a certain fixed percentage of its total power budget to the users.

IV. Performance Evaluation

For this work, we consider the following values for the number of UAVs and GUEs, $M_{uav} = 1$ and $M_{gue} = 1$, respectively. We consider a three-sectored AP equipped with three ULAs, having their respective boresights separated by $120°$ from one another. The users (UAV and GUE), who are randomly positioned on the grid within the coverage area of only one sector, are served by the AP. Two values of N are considered during the simulations, namely, $N = 4$ or $N = 8$ antennas. The operating frequency is set to 2 GHz. The AP power budget is 30 dBm and the antenna tilt (ϕ_{tilt}) was fixed at $20°$. The heights of the GUE and AP are set at 1.5 m and 11.5 m, respectively. The height of the UAV, on the other hand, is uniformly distributed between 23 m and 230 m.

In the considered scenario with $M = 2$ ($M_{uav} = 1$ and $M_{gue} = 1$), a δ factor is used to balance the power distribution between the two beams (one for the UAV and another for the GUE), where $0 < \delta < 1$.

In the first simulation scenario, in which a monobeam transmission was considered, a beam was directed towards the UAV, and then, in a second set of simulations, towards the GUE. Analyzing the cumulative distribution function (CDF) of the SINRs, in Figs. 2 and 3, it is evident that the direction of the beam impacts the signal performance. When the beam is facing the UAV, it is more favored, when the beam is facing the GUE, the opposite occurs, as expected. It is also important to highlight that the greater probability of transmission in the LOS condition for the UAV favors the increase in SINR.

In the next configuration, now employing the multibeam approach, we adjusted the power distribution factor δ to 0.3. In Fig. 4, we see that the GUE performance for $\delta = 0.3$ is better than that of the UAV. This shows that it is possible to prioritize a certain user (or group of users) by correctly balancing the power allocation. Then, we studied the case with a δ factor of 0.5, shown in Fig. 5. For the case of $\delta = 0.5$,

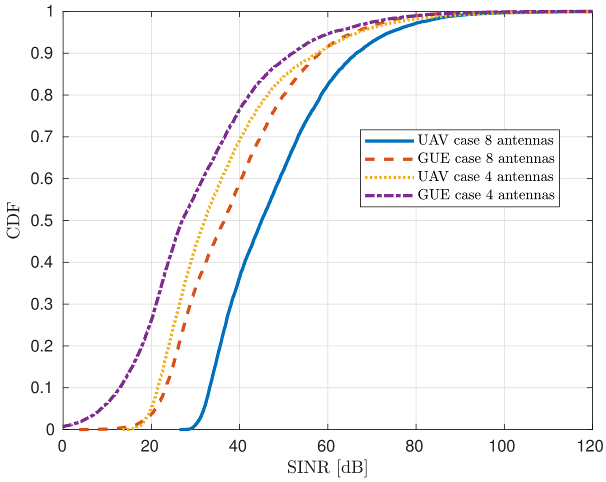

Fig. 2: CDF of SINR: beam towards the UAV.

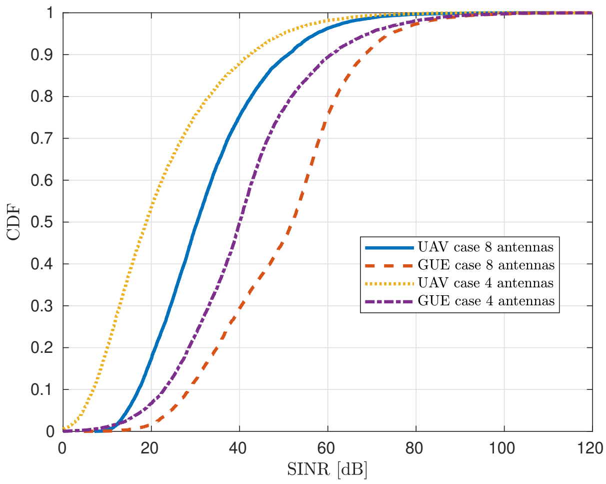

Fig. 3: CDF of SINR: beam towards the GUE.

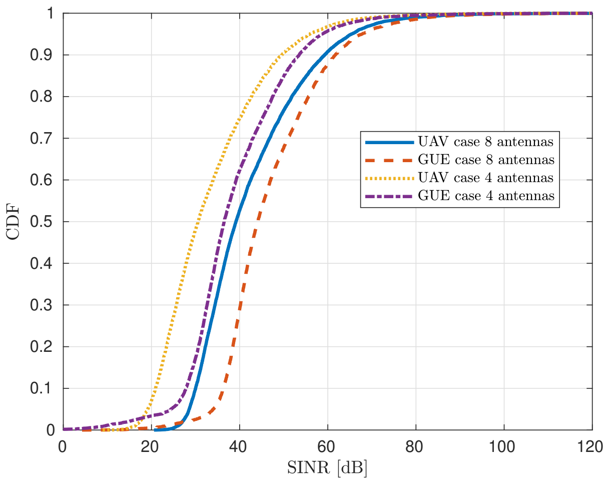

Fig. 4: CDF of SINR for multibeam with $\delta = 0.3$.

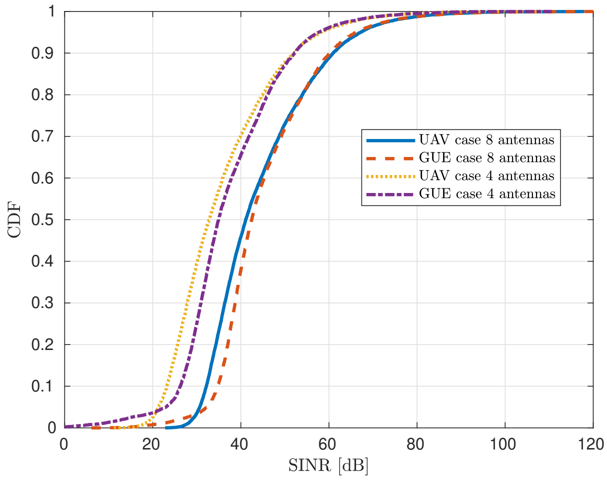

Fig. 5: CDF of SINR for multibeam with $\delta = 0.5$.

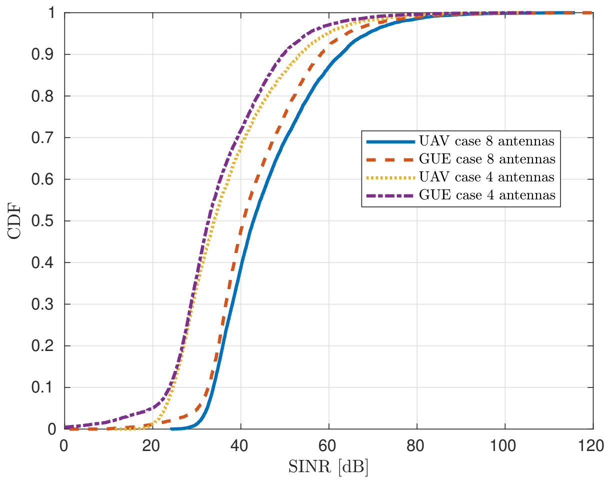

Fig. 6: CDF of SINR for multibeam with $\delta = 0.7$.

both users had similar performance, indicating that an equal power allocation in the considered multibeam scenario leads to a balanced performance. Finally, the δ factor was set to 0.7. In this scenario, it is observed that the UAV performed better than the GUE, as illustrated in Fig. 6.

All simulations were carried out for $N = 4$ antennas and $N = 8$ antennas. For situations of $N = 8$ antennas, as it can be seen in Figs. 2 to 6, users had superior performance compared to the scenario of $N = 4$ antennas, as expected.

V. Conclusions

Based on the simulation results, we can conclude that power allocation and beam direction significantly impact the SINR for both the UAV and the GUE. The impact of tuning power allocation δ is evident in multibeam configurations. When we allocate greater power to the GUE, this allocation results in a higher SINR for the GUE. On the other hand, reversing the power allocation to favor UAV leads to a higher SINR for the UAV. This result highlights the dynamic nature of power management in optimizing communication quality.

In Table II, we can see the SINR results obtained for different percentiles. Observing the results for the $\delta = 0.5$ allocation, we can see a similarity in the SINR values at the 50-th and 90-th percentiles, indicating that a uniform distribution of δ leads to balanced performance.

We can also highlight the influence on the number of antennas: with more antennas, there was an improvement in users'

TABLE II:
PERCENTILES FOR $N = 4$ AND $N = 8$ ANTENNAS

BEAM TOWARDS THE UAV				
PERCENTILE	UAV ($N = 4$)	GUE ($N = 4$)	UAV ($N = 8$)	GUE ($N = 8$)
10th	27.92 dB	12.86 dB	34.67 dB	26.44 dB
50th	34.08 dB	28.49 dB	45.13 dB	36.32 dB
90th	59.59 dB	52.12 dB	67.05 dB	54.40 dB
BEAM TOWARDS THE GUE				
10th	10.17 dB	22.88 dB	12.10 dB	36.33 dB
50th	18.79 dB	39.31 dB	26.35 dB	52.13 dB
90th	41.99 dB	59.60 dB	47.06 dB	68.60 dB
MULTIBEAM FOR $\delta = 0.3$				
10th	20.92 dB	21.90 dB	29.99 dB	31.23 dB
50th	30.56 dB	36.48 dB	39.15 dB	44.09 dB
90th	49.55 dB	57.09 dB	65.98 dB	68.77 dB
MULTIBEAM FOR $\delta = 0.5$				
10th	23.23 dB	18.75 dB	32.15 dB	28.43 dB
50th	36.78 dB	34.93 dB	43.13 dB	42.45 dB
90th	56.50 dB	52.15 dB	68.70 dB	65.12 dB
MULTIBEAM FOR $\delta = 0.7$				
10th	24.40 dB	13.50 dB	33.75 dB	27.60 dB
50th	36.90 dB	30.57 dB	44.29 dB	43.50 dB
90th	58.20 dB	53.15 dB	69.68 dB	62.78 dB

SINRs in all δ tuning scenarios, indicating better performance that can be explored with a large number of antennas. Thus, given the proposals for the future of mobile communications, the results of this study suggest that this strategic allocation of resources can be an appropriate tool to meet specific communication requirements in innovative scenarios, such as applications in agricultural monitoring, aerial surveillance and food delivery, leading to better efficiency in these new wireless scenarios.

REFERENCES

[1] P. Chandhar, D. Danev, and E. G. Larsson, "Massive MIMO for communications with drone swarms," *IEEE Transactions on Wireless Communications*, vol. 17, no. 3, pp. 1604–1629, 2017.

[2] G. Geraci, A. Garcia-Rodriguez, L. G. Giordano, D. López-Pérez, and E. Björnson, "Understanding UAV cellular communications: From existing networks to massive MIMO," *IEEE Access*, vol. 6, pp. 67853–67865, 2018.

[3] M. C. R. Lobão, W. O. Feitosa, R. P. Antonioli, Y. C. B. Silva, W. C. Freitas Jr, and G. Fodor, "On the impact of antenna tilt on cell-free systems serving ground users and UAVs," in *XL Simpósio Brasileiro de Telecomunicações e Processamento de Sinais*, 2023.

[4] ITU-R, "Guidelines for evaluation of radio interface technologies for IMT-advanced," *ITU Report*, vol. 638, no. 31, 2009.

[5] C. D'Andrea, A. Garcia-Rodriguez, G. Geraci, L. G. Giordano, and S. Buzzi, "Analysis of UAV communications in cell-free massive MIMO systems," *IEEE Open Journal of the Communications Society*, vol. 1, pp. 133–147, 2020.

[6] 3GPP, "Enhanced LTE support for aerial vehicles, 3rd Generation Partnerhsip Project," vol. 15.0.0., Jan. 2018.

[7] 3GPP, "Study on channel model for frequencies from 0.5 to 100 GHz, 3rd Generation Partnership Project," vol. 17.0.0., Jan. 2018.

[8] C. A. Balanis, *Antenna theory: analysis and design*. John wiley & sons, 2016.

[9] Y. Luo, J. A. Zhang, W. Ni, J. Pan, and X. Huang, "Constrained multibeam optimization for joint communication and radio sensing," *IEEE Global Communications Conference (GLOBECOM)*, pp. 1–6, 2019.

[10] J. A. Zhang, X. Huang, Y. J. Guo, J. Yuan, and R. W. Heath, "Multibeam for joint communication and radar sensing using steerable analog antenna arrays," *IEEE Transactions on Vehicular Technology*, vol. 68, no. 1, pp. 671–685, 2018.